Albacore (*Thunnus alalunga*) fishing ground in relation to oceanographic conditions in the western North Pacific Ocean using remotely sensed satellite data

MUKTI ZAINUDDIN,[1,*] KATSUYA SAITOH[2] AND SEI-ICHI SAITOH[3]

[1]*Faculty of Marine Science and Fisheries, Hasanuddin University, Jl. P. Kemerdekaan, KM 10, Tamalanrea, Makassar, 90245, Indonesia*
[2]*Japan Fisheries Information and Service Center (JAFIC), 2-9-7 Ikenohata Taito-ku, Tokyo 110-0008, Japan*
[3]*Laboratory of Marine Environment and Resource Sensing, Graduate School of Fisheries Sciences, Hokkaido University, 3-1-1 Minato-cho, Hakodate, Hokkaido 041-8611, Japan*

ABSTRACT

Satellite-based oceanographic data of sea surface temperature (SST), sea surface chlorophyll-a concentration (SSC), and sea surface height anomaly (SSHA) together with catch data were used to investigate the relationship between albacore fishing ground and oceanographic conditions and also to predict potential habitats for albacore in the western North Pacific Ocean. Empirical cumulative distribution function and high catch data analyses were used to calculate preferred ranges of the three oceanographic conditions. Results indicate that highest catch per unit efforts (CPUEs) corresponded with areas of SST 18.5–21.5°C, SSC 0.2–0.4 mg m^{-3}, and SSHA −5.0 to 32.2 cm during the winter in the period 1998–2000. We used these ranges to generate a simple prediction map for detecting potential fishing grounds. Statistically, to predict spatial patterns of potential albacore habitats, we applied a combined generalized additive model (GAM)/generalized linear model (GLM). To build our model, we first constructed a GAM as an exploratory tool to identify the functional relationships between the environmental variables and CPUE; we then made parameters out of these relationships using the GLM to generate a robust prediction tool. The areas of highest CPUEs predicted by the models were consistent with the potential habitats on the simple prediction map and observation data, suggesting that the dynamics of ocean eddies (November 1998 and 2000) and fronts (November 1999) may account for the spatial patterns of highest albacore catch rates predicted in the study area. The results also suggest that multispectrum satellite data can provide useful information to characterize and predict potential tuna habitats.

Key words: albacore, generalized additive model, generalized linear model, potential habitat, satellite data, simple prediction map, western North Pacific Ocean

INTRODUCTION

The area of interest for this study is the western North Pacific Ocean, extending from 25°N to 45°N, and from 140°E to 180°E (Fig. 1). This region where the warm Kuroshio Current and the cold Oyashio Current meet is one of the most productive tuna fishing grounds in the world. The interaction of these two currents form a region called the Transition Zone (Roden, 1991) in the western North Pacific Ocean. There are two remarkable oceanographic fronts bounding the transition zone, at approximately 32°N (Subtropical Front) and 42°N (Subarctic Front), where several physical oceanographic structures such as fronts and eddies occur (Roden, 1991). Dynamics of these oceanographic structures are key to sustaining a highly productive habitat into which various ecologically and commercially pelagic species, including albacore tuna, migrate for feeding (Uda, 1973; Polovina *et al.*, 2001).

Albacore, *Thunnus alalunga*, is the main target species of the Japanese longline fishery in the study area. Albacore occur between 10°N and 50°N in the North Pacific and migrate widely from an area surrounding the Japanese Islands to the west coast of the United States (Laurs and Lynn, 1991). This species spawns in summer near the North Equatorial Counter Current region between 10°N and 20°N, south of the subtropical convergence (Laurs and Lynn, 1991;

*Correspondence. e-mail: mukti_fishocean@yahoo.co.id
Received 2 August 2004
Revised version accepted 26 March 2006

 doi:10.1111/j.1365-2419.2008.00461.x

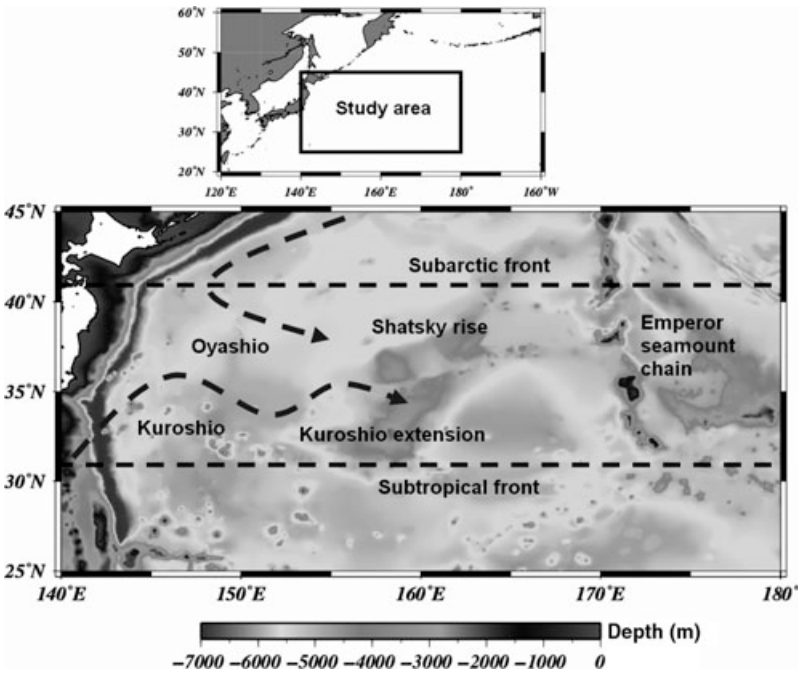

Figure 1. A geographic location and bathymetry of the study area in the western North Pacific Ocean.

Kimura *et al.*, 1997). Albacore are also believed to perform a transpacific migration (Kimura *et al.*, 1997), and understanding of the dynamics of high productive tuna habitat is of interest. Although the study area is one of the most productive fishing grounds and has a long history of tuna exploitation, little is known about underlying oceanographic features affecting the spatial dynamics of albacore distribution and abundance.

Remotely sensed satellite observations of sea surface may provide significant information to assess and improve the potential yield of fishing grounds. Polovina *et al.* (2001) concluded that ocean color features are good indicators of oceanic fronts as indicated by 0.2 mg m^{-3} surface chlorophyll-a (chl-a) density (known as the Transition Zone Chlorophyll Front – TZCF) estimated from SeaWiFS in the central-eastern North Pacific where albacore were using the front as a migration route and as a forage habitat. Laurs *et al.* (1984) used satellite images of SSC Nimbus/CZCS and SST NOAA/AVHRR to relate albacore catch and oceanographic features in the eastern Pacific and found that being near the ocean color and thermal fronts appeared to be necessary for fishing success. However, recent studies stated that the spatial relationship between bluefin tuna distribution and SST fronts is inconsistent in the Gulf of Maine (Schick *et al.*, 2004) and spatial distribution patterns of yellowfin tuna CPUE are not related to satellite-derived SST conditions (e.g., Montañez *et al.*, 2004).

Most investigations dealing with oceanographic factors related to catch data are concerned with the correlation of a single parameter with spatial and temporal tuna distributions. Tuna distribution and abundance are sensitive to variability of environments and associate strongly with the high density of forage (e.g., Sund *et al.*, 1981; Lehodey *et al.*, 1997). It is most likely that albacore respond synoptically to a number of environmental factors. Thus, it is important to combine several environmental factors, which might provide new insight into detecting the high-density tuna forage areas and thus potential fishing grounds (tuna habitats).

The objectives of the present study were to investigate the relationship between albacore fishing ground and oceanographic conditions and also to predict the areas with the highest probability of finding albacore (potential albacore habitats) in the western North Pacific Ocean using multispectrum satellite images.

DATA AND METHODS

In this paper, we used two types of data sets: fishery and satellite-based oceanographic data from 1998 to 2000. To meet the objectives of this study, we focused our analyses mostly over the period of high albacore abundance, i.e., winter period (November–March).

Fishery data

The fishery data consisted of daily albacore catch and longline fishing effort, fishing position in latitude and longitude for the period from January 1998 to December 2000 obtained from the Japan Fisheries Information and Service Center (JAFIC). These data were compiled into monthly resolved data. According to Andrade and Garcia (1999), the catch data were divided into three categories: null catches, positive catches, and high catches. For this study, we divided into three cases for albacore CPUE: (1) cases with CPUE equal to zero – 'null catches'; (2) cases with CPUE greater than zero but lower than 0.41 tons – 'positive catches'; and (3) cases with CPUE greater than 0.41 tons – 'high catches'. The value 0.41 tons represents the lower limit of the upper quartile of CPUEs greater than zero. In the present study, we used the high catch data analysis to estimate optimum ranges of three oceanographic variables during the winter period (November–March). For the high catch data, our preliminary study found a significant difference between the data distribution and the other distributions (positive and null catches) using a *t*-test.

Remotely sensed satellite data

Remotely sensed oceanographic data, specifically, sea surface temperature (SST), sea surface chl-a concentration (SSC), and sea surface height anomalies (SSHA) were derived from the Tropical Rainfall Measuring Mission (TRMM)/TRMM Microwave Imager (TMI), Orbview-2/SeaWiFS and TOPEX/POESIDON-ERS merged (AVISO), respectively. We used monthly TRMM/TMI SST data sets version 3a, extending from 40°S to 40°N at a pixel resolution of 0.25° (about 25 km) for both latitude and longitude, obtained from the Remote Sensing System database (http://www.remss.com). The TMI SSTs have been shown to agree well with SSTs measured with buoys and ships with a mean difference of ~0.1°C and a RMS difference of ~0.6°C (Wentz *et al.*, 2000; Bhat *et al.*, 2004). This sensor represents a satellite microwave sensor that is capable of accurately measuring SST under nearly all weather conditions (Wentz *et al.*, 2000). The TMI data are suitable for studying tuna distribution and migration, as they have a high accuracy and cover a distribution range of mostly albacore in the western North Pacific Ocean. As the spatial resolution of TRMM/TMI is 25 km, the SST images were resampled onto a 9-km grid to match with the SeaWiFS SSC data using the interactive data language (IDL) software package.

Sea surface temperature data derived from NOAA/AVHRR Pathfinder version 5.0 were also used to generate predictions of albacore CPUE during 1998–2000. We obtained global monthly data sets from http://podaac.jpl.nasa.gov/ (the NASA/JPL PO-DAAC Pathfinder database) with a spatial resolution of 4 km for both latitude and longitude. These data were also resampled to a lower spatial resolution (9 km) using the IDL. We selected these data to perform predicted CPUE over the entire range of the study area, as TMI SST data cover only the area through 40°N.

The Sea-viewing Wide Field-of-view Sensor (SeaWiFS) has provided high spatial and temporal data resolutions with the accuracy of chlorophyll estimations approximately 30–50% of ship observations (McClain *et al.*, 1998). This sensor has proved the key source of information to recent studies on fisheries oceanography in the eastern and central North Pacific (Polovina *et al.*, 2001). We used global area coverage, monthly composite SeaWiFS level 3 standard mapped images with a spatial resolution of about 9 × 9 km on an equidistant cylindrical projection.

The SSHA data were obtained from the Maps of Sea Level Anomalies (MSLA)/Archiving, Validation and Interpretation of Satellite Oceanographic Data (AVISO) scientific team of Collecte, Localisation, Satellite (CLS)/Centre National d'Etudes Spatiales (CNES) data center (http://www.jason.oceanobs.com/). The grided data are calculated by combining Topex/Poseidon and ERS altimeter data. The accuracy of these maps can be reduced to about 3 cm RMS on average as it has the very efficient correction of orbit errors on along-track data (Testut *et al.*, 2003). In this study, we used weekly high resolution SSHA and made a monthly composite map from the weekly data to identify eddy-like features and to estimate current magnitude and direction. We averaged the horizontal velocities (u and v geostrophic components) in the x and y directions to obtain more realistic estimates. The SSHA values (z) were used to calculate the east-west (dz/dx) and north-south (dz/dy) gradients, where x, y, and z are all in centimeters. These gradients were used for calculating the u and v components of both the geostrophic velocities and eddy kinetic energy (EKE) with 0.5° latitude and longitude resolution as follows (Polovina *et al.*, 1999; Robinson, 2004):

$$u = -\left(\frac{g}{f}\right)\frac{dz}{dy} \tag{1}$$

$$v = \left(\frac{g}{f}\right)\frac{dz}{dx} \tag{2}$$

$$\mathrm{EKE} = \left(\frac{1}{2}\right)\left(u^2 + v^2\right) \tag{3}$$

where g is the local acceleration due to gravity (980 cm s^{-2}) and $f = 2\Omega\sin\Phi$, where $\Omega = 7.29 \times 10^{-5}$ radians s^{-1} and Φ is latitude.

Generating a simple prediction map

Preferred oceanographic conditions were obtained by considering confidence ranges of both the high catch data (mean ± one standard deviation) and empirical cumulative distribution function (ECDF; the specific value of variables at D(t) max ± one standard deviation) during the winter period 1998–2000. We matched both these ranges to determine the preferred ranges of the three environmental conditions. A simple prediction map was computed by combining the three favorable oceanographic ranges (SST, SSC, and SSHA) into a single map with the same spatial and temporal scale for each grid data using the IDL. This map consisted of binary output in which the white color represents a predicted area (potential fishing ground), and the blue color denotes a low probability area in which to find albacore. Catch data were then superimposed on the map, and the high CPUEs were compared graphically with the predicted area.

Using ECDF, we analyzed the stronger association between the three oceanographic variables and albacore CPUE during the same period. In this analysis, we used three functions (Perry and Smith, 1994; Andrade and Garcia, 1999) as follows:

$$f(t) = \frac{1}{n}\sum_{i=1}^{n} l(xi) \tag{4}$$

with the indicator function

$$\begin{aligned} l(xi) &= \begin{cases} 1 & \text{if } xi \le t \\ 0 & \text{otherwise} \end{cases} \\ g(t) &= \frac{1}{n}\sum_{i=1}^{n} \frac{yi}{\bar{y}}\, l(xi) \end{aligned} \tag{5}$$

$$D(t) = \max\left|f(t) - g(t)\right| \tag{6}$$

where $f(t)$ is empirical cumulative frequency distribution function, $g(t)$ is catch-weighted cumulative distribution function, $l(xi)$ is indication function, and $D(t)$ is the absolute value of the difference between the two curves $f(t)$ and $g(t)$ at any point t, and assessed by the standard Kolmogorov–Smirnov test. n is the number of fishing trips, xi the measurement for satellite-derived oceanographic variables in a fishing trip i, t an index ranking the ordered observations from the lowest to highest value of the oceanographic variables, yi the CPUE obtained in a fishing trip i, and $\bar{y}$ the estimated mean of CPUE for all fishing trips. The coordinate labeled 'max' represents the specific value of the variables at which the difference between the two curves ($|g(t) - f(t)|$) was maximum.

Contour map

Contour maps were created using the mean (center) values of the preferred oceanographic variables (i.e., 20°C SST, 0.3 mg m^{-3} SSC, and 13 cm SSHA). These values represent the strongest association between environment and CPUE. The contour lines were overlain on SSHA images to assess the oceanographic features controlling albacore abundance. The specific SSHA contour level depicted was compared with the EKE map to identify eddy fields near fishing locations. The relationship between the distance of the SST and SSC contour lines and CPUE was examined, and was used to detect the possible occurrence of frontal zones. The contour lines and all maps presented in this work were created using the generic mapping tool software package.

Statistical models for spatial prediction

To predict spatial patterns of potential albacore habitats, statistical models were applied. Our models were built by combining a generalized additive model (GAM) and generalized linear model (GLM). We constructed the GLM based on the trend of albacore CPUE in relation to the predictors resulting from a GAM with the least different residual deviance (Mathsoft, 1999). A GAM is a non-parametric generalization of multiple linear regressions which is less restrictive in assumptions of the underlying statistical data distribution (Hastie and Tibshirani, 1990). The GAM was used to determine the nature of the relationship between CPUE and the environmental variables. Although the GAM may explain the variance of CPUE more effectively and flexibly than the GLM, the model has no analytical form (Mathsoft, 1999). A GLM provides a way of estimating a function of mean response (CPUE) as a linear function of some set of covariates (predictors). Thus, in our analyses, we used the GLM fit to predict a spatial pattern of albacore CPUE.

We first constructed a GAM as an exploratory tool to identify the shapes of the relationships between environmental factors and CPUE as it was most likely that the expected relationships are non-linear. Once the shape of the relationships between the response

variable and each predictor was identified, the appropriate functions were used to parameterize these shapes in the GLM model. The GLM was used to generate a robust predictive equation. The shapes resulting from the GAM were reproduced as closely as possible using the piecewise GLM. Three environmental variables were included in the analysis using a GAM (equation 7) and a GLM (equation 8), as follows:

$$\mathrm{Ln}(\mathrm{CPUE}+1) = \mathrm{a} + s(\mathrm{SST}) + s(\mathrm{SSC}) + s(\mathrm{SSHA}) + \mathrm{e} \quad (7)$$

$$\mathrm{Ln}(\mathrm{CPUE}+1) = \mathrm{b} + \mathbf{b1}(\mathrm{SST}) + \mathbf{b2}\mathrm{Ln}(\mathrm{SSC}) + \mathbf{b3}(\mathrm{SSHA}) + \mathrm{e} \quad (8)$$

where a and b are constants, $s(\cdot)$ is a spline smoothing function of the variables (SST, SSC, and SSHA) and e is a random error term, and $\boldsymbol{b_1}$, $\boldsymbol{b_2}$, and $\boldsymbol{b_3}$ are the vectors of model coefficients.

Albacore CPUEs follow a continuous distribution; we fit the GLM using a Normal distribution as the family associated with identity link function (McCullagh and Nelder, 1989). The data distribution and the link function in the GLM were exactly the same as those used in the GAM. A logarithmic transformation of the CPUE was used to normalize asymmetrical frequency distribution, and we added a value of one to all CPUE values to account for zero CPUE data. The model selection process for the best predictive model for explaining CPUE data was based on a forward and backward stepwise manner. The predictors were considered to be significant for explaining the variance of CPUE, if the residual deviance and Akaike Information Criteria (AIC) decrease with each addition of the variables and the probability of final set of variables was lower than 0.01 ($P < 0.01$).

RESULTS

Seasonal variability of CPUE and oceanographic conditions

The temporal variability of CPUE and oceanographic conditions (SST, SSC, and SSHA) throughout the years from 1998 to 2000 was very similar (Fig. 2). The high albacore catches were found during the winter (November–March) (Fig. 2a) where fishing sets were carried out in warm water SST (Fig. 2b), with relatively high SSC (Fig. 2c) and SSHA (Fig. 2d). In contrast, the relatively low CPUEs were obtained during the summer (April–October) when fishing

Figure 2. Temporal variability of CPUE of albacore fishery (a), TRMM/TMI SST (b), SeaWiFS SSC (c), and AVISO SSHA (d) extracting from fishing ground from 1998 to 2000.

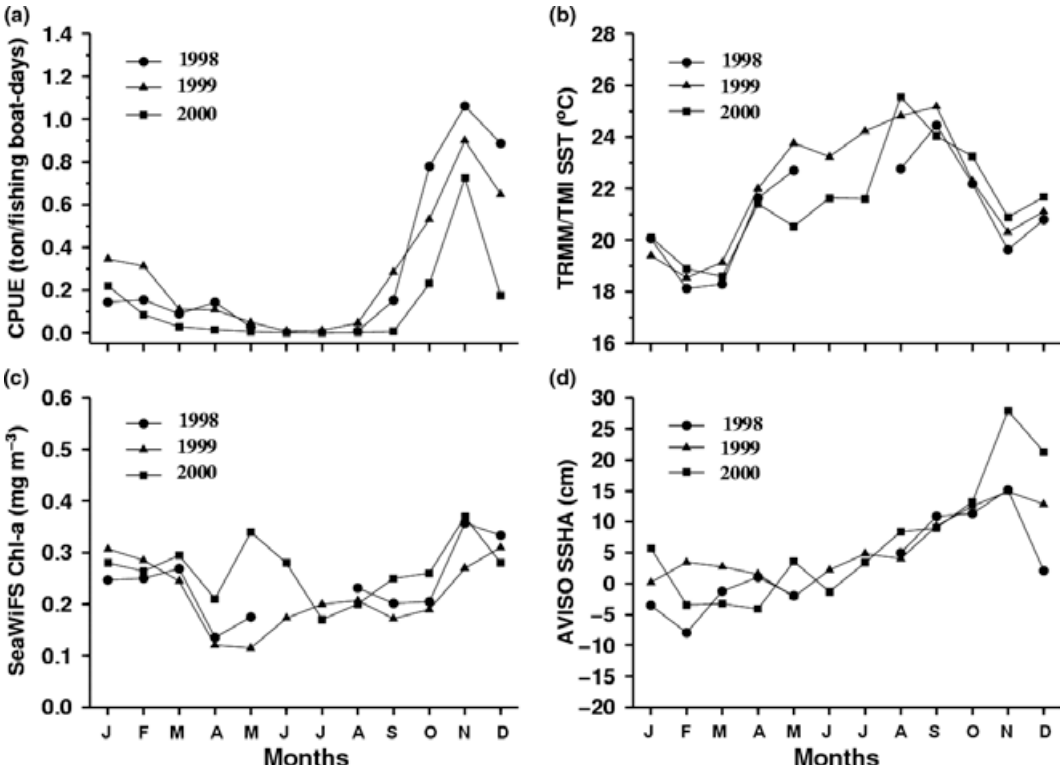

effort occurred in areas of relatively high SST, and relatively low SSC and SSHA. Hence, we defined the summer and the winter periods based on the variability of these oceanographic conditions.

The peaks of catch always occurred in the winter period, particularly in November. The highest CPUEs in this month occurred in areas of relatively warm water of SST near 20°C (Fig. 2b), relatively high SSC of about 0.3 mg m^{-3} (Fig.2c) and SSHA of about 13 cm (Fig. 2d). Albacore were mainly taken in lower numbers, where the oceanographic conditions of SST, SSC, and SSHA were higher than 22°C, lower than 0.2 mg m^{-3}, and lower than 10 cm, respectively (Fig. 2).

Figure 3 shows the variation in SST and SSC from 145°E to 180°E along 36°N latitude during 1998–2000. 36°N has been found as a center of albacore fishing ground by latitude from our preliminary study. The specific SSC of 0.3 mg m^{-3} is more pronounced from November to March, while the SST of 20°C occurred during November–December. These data indicated that the most productive habitat occurred from November to December and then was followed by the period of January–March. The less productive fishing grounds in this area occurred from June through September and had relatively high SST and relatively low SSC.

Preferred oceanographic conditions for albacore

The fishing sets of high catch of albacore in the winter period occurred in areas where SST ranged from 16°C to 23°C (Fig. 4a). However, most catches were obtained in areas where SST varied primarily between 18.5°C and 21.5°C (20.0 ± 1.5°C). The highest CPUEs in fishing grounds tended to be centered at 20°C SST.

Figure 3. Isopleth of the TRMM/TMI SST and the SeaWiFS SSC data distribution along latitude 36°N during 1998–2000.

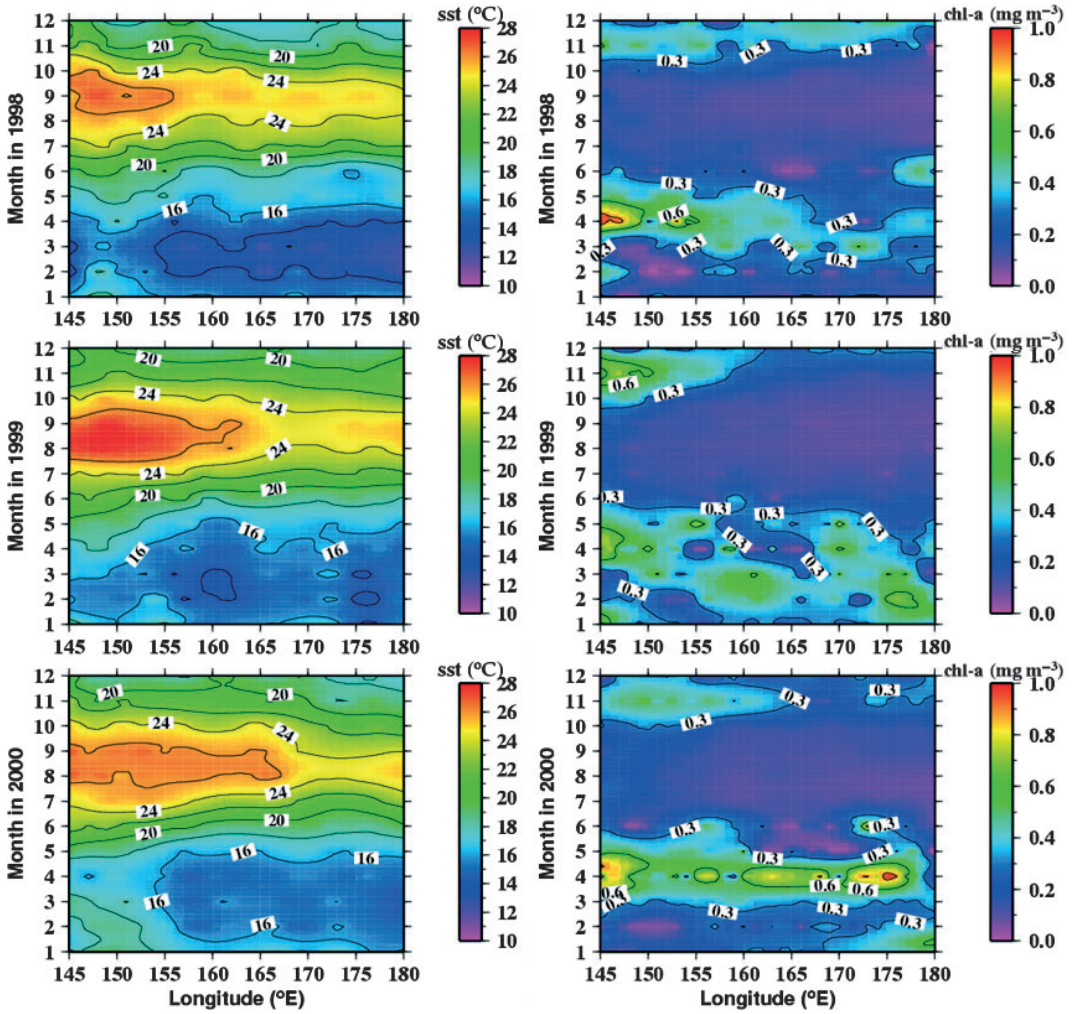

Figure 4. Relationship between environmental variables of TRMM/TMI SST (*a*), SeaWiFS SSC (*b*) and AVISO SSHA (*c*) and fishing frequency of high catch data for albacore during winter period 1998–2000.

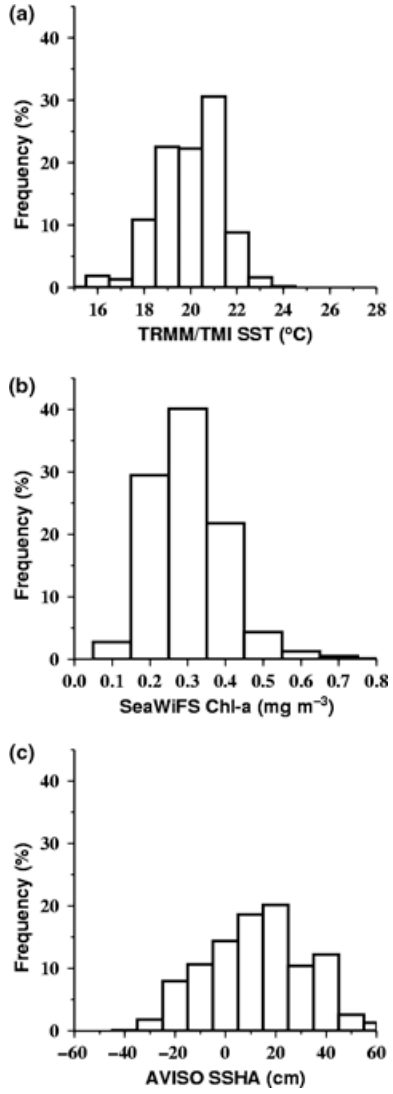

The frequency of fishing days of high catch of albacore in relation to SSC follows a Gaussian distribution. The fishing sets occurred in areas where SSC varied from 0.05 to 0.7 mg m^{-3}. However, albacore catches were mostly taken in fishing grounds where SSC ranged from 0.2 to 0.4 mg m^{-3} (0.3 ± 0.1 mg m^{-3}) (Fig. 4b). The histogram of high catch rates showed that fishing efforts most frequently occurred at 0.3 mg m^{-3} surface chl-a concentration.

Distribution of high CPUEs in relation to SSHA indicated that albacore were found in fishing grounds from about −35 to 65 cm SSHA. Most of the fish were obtained in areas where SSHA ranged from −6.8 to 33.2 cm (13.2 ± 20.0 cm) (Fig. 4c). The center of the SSHA range was found at 13.2 cm.

Using the ECDF, the relationship between CPUE and the three environmental variables reinforces the results obtained above (Fig. 5). The cumulative distribution curves of the variables are different and the degrees of the difference between two curves (D(*t*)) are highly significant ($P < 0.01$). The results showed a stronger association between CPUE and the variables, with SSC ranging from 0.2 to 0.4 mg m^{-3} (Fig. 5a), SST ranging from 18.5°C to 20.5°C (Fig. 5b) and SSHA ranging from −5.0 to 32.2 cm (Fig. 5c). The strongest associations between CPUE and the three variables occurred at 20.3°C SST, 0.3 mg m^{-3} SSC and 13.6 cm SSHA, respectively. Albacore catch rates tended to decrease in areas of outside those favorable ranges.

Based on these results, the preferred oceanographic conditions for albacore were obtained in areas of SST 18.5–20.5°C, SSC 0.2–0.4 mg m^{-3}, and SSHA −5.0 to 32.2 cm. The optimum values of these ranges were found at 20°C SST, 0.3 mg m^{-3} SSC, and 13 cm SSHA, respectively.

Simple predicted area of potential fishing ground

The simple prediction map showed that in November 1998, potential fishing grounds occurred in the areas near 34°–38°N and 164°–170°E (Fig. 6). The predicted area of occurrence was wider in November 1999 than in 1998 and was mainly associated with the productive albacore fishery in the location of 160°–172°E and that of 35°–38°N. In November 2000, potential fishing grounds well formed between 35°N and 37°N, and 162°E and 166°E and the albacore fishery strongly concentrated near that area.

Estimated contour and EKE maps

Altimetry data revealed that albacore fisheries were mostly concentrated in areas of positive SSHA near a contour level of 13 cm and relatively high EKE (Fig. 7). These results indicated that albacore habitat developed near the eastern Shatsky Rise area, northern Kuroshio Extension (KE), over the anticyclonic eddy from 36°N to 38°N and from 167°E to 169°E in November 1998, and from 35°N to 37°N and from 167°E to 169°E in November 2000. In November 1999, the catchability of albacore was found to be associated with slightly positive SSHA but was not associated with relative high EKE. It is interesting to note that the albacore CPUEs were significantly increased where the distance of latitudinal mean position between the contour levels of SST 20°C and the SSC 0.3 mg m^{-3} was small (Figs 7 and 8). The relationship showed a

Figure 5. Empirical cumulative distribution frequencies for (a) SeaWiFS SSC, (b) TRMM/TMI SST, and (c) AVISO SSHA, and SST, SSC and SSHA as weighted by albacore catch during the winter period 1998–2000.

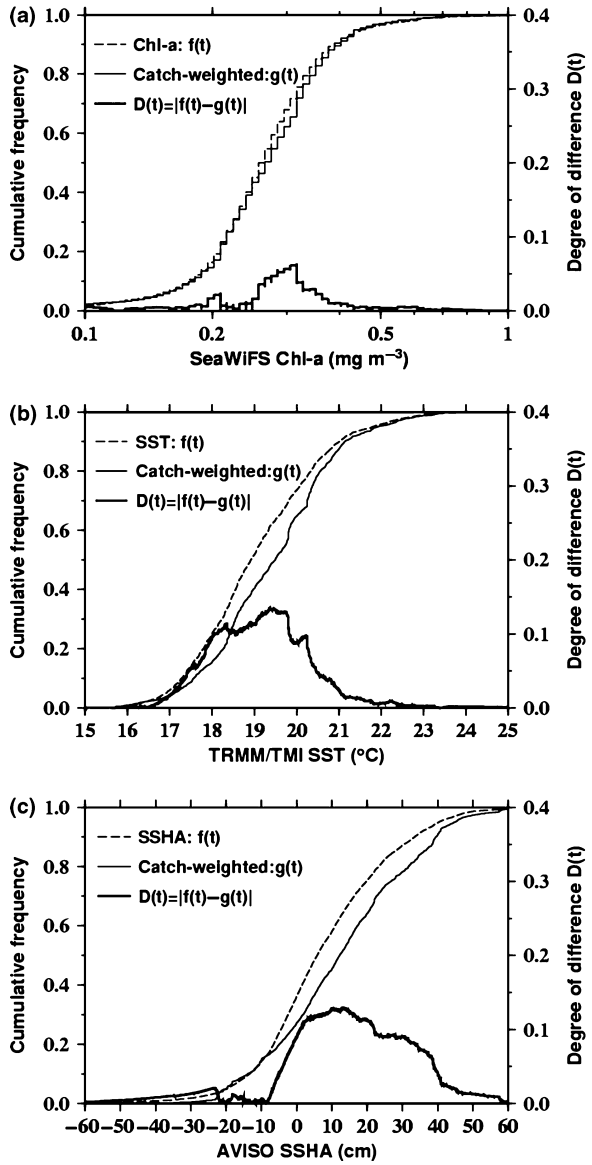

high determinant coefficient (R^2 = 0.80) and was highly significant ($P < 0.01$) (Fig. 8). It is clearly shown that the albacore fishery was aggregated in areas from 35°N to 37°N and from 162°E to 168°E where SST 20°C and the 0.3 mg m^{-3} SSC occurred in November 1999.

Spatial prediction of albacore CPUE by statistical model

The relationship between albacore CPUE and all three variables was highly significant ($P < 0.0001$) using the GAM. With each addition of the variables

Figure 6. The spatial distribution of albacore CPUE (ton/fishing-boat days) from longline fishery in November from 1998 to 2000 overlain on simple prediction maps generated from a combination of TRMM/TMI SST, SeaWiFS SSC and AVISO SSHA satellite data.

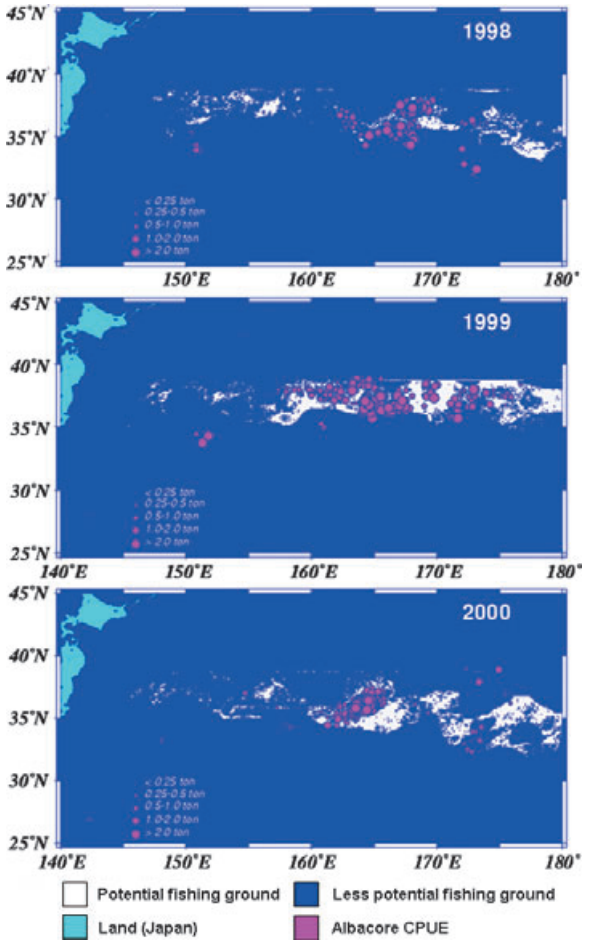

selected to represent subsequent periods, the residual deviance decreased and the cumulative variance increased, indicating increasingly better model fit and parsimony using the three oceanographic variables (Table 1). Albacore catches were found in strong association with environmental SST of about 18.5–21.5°C, SSC of about 0.2–0.4 mg m^{-3} and SSHA of about −5 to 40 cm (Fig. 9). These results were consistent with the output producing from the ECDF and high catch histogram analyses.

Similar to the GAM results, the analysis deviance table shows that each predictor in the GLM was statistically significant ($P < 0.0001$; Table 2). Using the GLM, we found that the addition of each additional variable chosen to represent subsequent periods resulted in lower residual deviance and AIC, indicating that all variables contribute significantly to the

Figure 7. Spatial distribution of albacore CPUE (ton/fishing-boat days) from Japanese longline fishery (dots) in November from 1998 to 2000 superimposed on (*left*) SSHA map with contour lines of 20°C SST isotherm, the 0.3 mg m^{-3} SSC isopleth and 13 cm SSHA and, (*right*) EKE map.

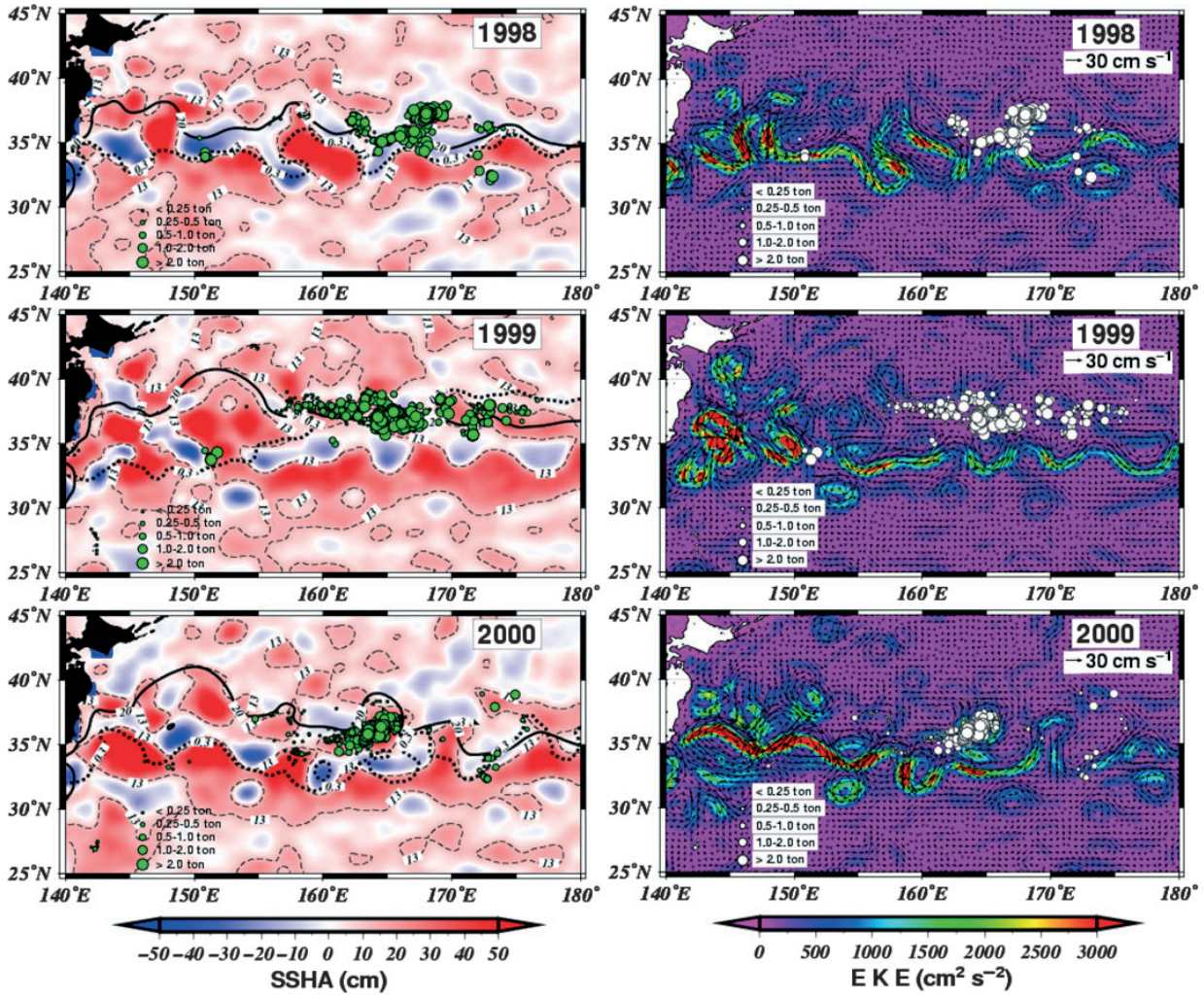

better model fit. The GLM deviance (~2.25%) was significantly less than that of the GAM. We used the GLM fit to predict albacore CPUE over the entire study area.

Our models showed that the areas of high albacore CPUEs agree well with the potential habitats on the simple prediction map and observation data (Fig. 10). Despite catch rates predicted by the GLM being lower than fishery data, it is clear that the locations of high CPUE prediction coincided with the potential productive albacore fishery near 35°–38°N and 165°–170°E in November 1998, 36°–38°N and 164°–172°E in November 1999, and 35°–37°E and 162°–165°E in November 2000. For that period, it is clear that the transition zone of western North Pacific Ocean (30–40°N) is a productive tuna fishing ground. The northern and southern parts of this region were found to be areas of less productive tuna fishing ground.

DISCUSSION

Although this study used short time series data sets (1998–2000), we have selected the biophysical environmental data to accurately describe the environment around albacore fishing grounds. The TMI SST was selected as the microwave sensor is capable of measuring SST through clouds. A combination of these data with the SeaWiFS SSC and altimetry SSHA data, which have proved to key in detecting potential forage habitats for pelagic species (Polovina *et al.*, 2001, 2004), was thought to be consistent for analysis. As a result, our findings could be understood

Figure 8. The relationship between albacore CPUE and the distance of mean position between the 20°C SST isotherm and the 0.3 mg m^{-3} SSC isopleth contour lines by latitude (°N) from 160°E to 180° in winter period during 1998–2000.

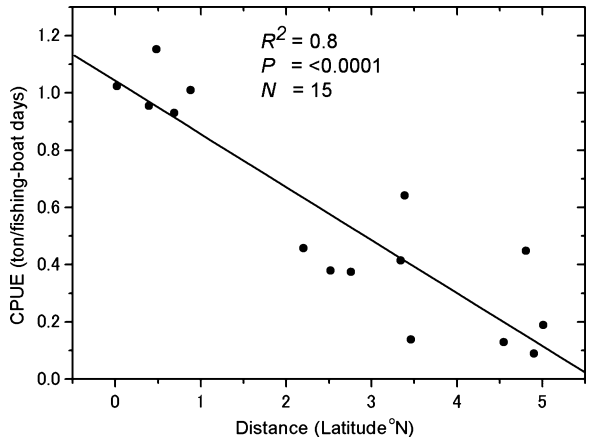

Table 1. Residual deviance and cumulative variance of albacore CPUE explained in GAM with variables added sequentially (first to last).

Variable	Residual d.f.	Residual deviance	Cumulative variance
Mean	1457	275.9598	
SST	1453	265.1950	3.9%
SSC	1449	248.4326	10.0%
SSHA	1445	229.5128	16.8%

Table 2. Construction of the GLM – as each variable is added, residual deviance, the approximate AIC, and *F*-statistic are examined to find significantly predictors.

Variable	Residual d.f.	Residual deviance	AIC	*F*
NULL	1457	275.95	276.34	
SST	1456	270.08	262.78	36.21
SSC	1455	252.99	249.29	105.47
SSHA	1454	235.72	237.23	106.54

as a preliminary insight into detecting and predicting potential albacore habitat. The relationship between albacore catch and environments clearly indicates that there are specific times and locations where albacore are abundant (Fig. 2). The increased albacore CPUEs mostly occur in the winter period and associate with the potential predicted areas. In this period, albacore have a tendency to concentrate near favorable oceanographic conditions (Fig. 4) which probably represent good feeding opportunities. These preferred conditions may stimulate a potential habitat especially during November–December where albacore use this area as a feeding area and as a migration path (Polovina *et al.*, 2001).

In contrast, during the summer period, albacore fishing grounds were poorly developed, which is indicated by relatively high SST (greater than 22°C), relatively low SSC (less than 0.2 mg m^{-3}), and moderate SSHA (nearly 0 cm). In this period, albacore tend to disperse widely as they encounter less favorable oceanographic conditions. As a result, catch rates for the albacore fishery over the study area tended to be low. During this period, albacore may conduct a transpacific migration to the eastern Pacific Ocean from approximately June to August (Fig. 3). It is likely that this behavior was carried out to search for potential forage habitats in the eastern North Pacific Ocean to fulfill a high energetic requirement (Olson and Boggs, 1986).

In the present study, we describe a highly productive albacore habitat that is strongly linked to dynamics of physical oceanographic structures such as ocean eddies, frontal zones, and the Kuroshio and Oyashio currents. This study shows that the highest CPUEs correspond to the areas of 18.5–21.5°C SST, 0.2–0.4 mg m^{-3} SSC, and −5 to 32 cm SSHA (Figs 4 and 5); hence, these areas were referred to as potential habitats for albacore. It is interesting to note that these biologically important areas can be plotted out over a map to detect their spatial patterns. Based on our results, the most productive fishing grounds for albacore strongly formed over the potential habitats during November 1998–2000 (Fig. 6). Albacore distributions associate clearly with the spatial patterns of the productive habitat in every year. We consider those areas as forage habitats where food concentrations preferred by albacore may well be enhanced. Therefore, the three environmental factors could be regarded as reasonable indices of the environmental conditions used to locate areas with highest probability of finding albacore. Our results suggest that the potential habitat structures could be reasonable proxies indicating the position of important physical oceanographic features such as ocean eddies and fronts in the study area.

The strongest affinities for tuna aggregation within the productive habitat were characterized by SST of about 20°C, SSC of about 0.3 mg m^{-3}, and 13 cm SSHA (Figs 4 and 5). These results are very similar to the previous study for albacore tuna in relation to SST (Uda, 1973) and SSC (Polovina *et al.*, 2001) in the western and central North

Figure 9. Generalized additive model (GAM) derived effect of oceanographic variables (a) TRMM/TMI SST, (b) SeaWiFS SSC, and (c) AVISO SSHA on albacore CPUE (log transformed). Dashed lines indicate 95% confidence intervals. The relative density of data points is shown by the rug plot on the *x*-axis.

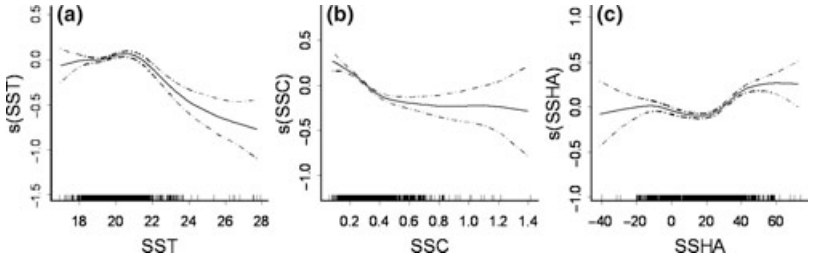

Figure 10. The spatial distribution of albacore CPUE (ton/fishing-boat days) from longline fishery in November from 1998 to 2000 overlain on predicted CPUE by the GLM using the three predictors (NOAA/AVHRR SST, SeaWiFS SSC, and AVISO SSHA).

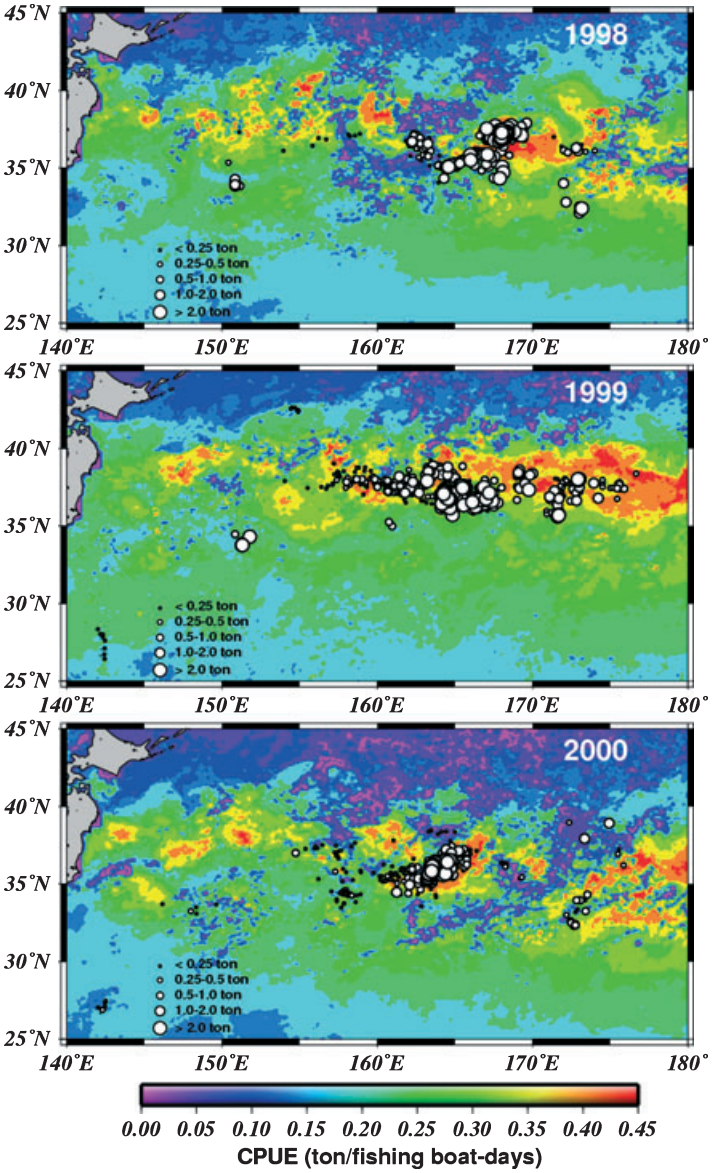

Pacific. In the winter period, the increased fishing success associates with southward oscillations of both 0.3 mg m^{-3} SSC isopleth and 20°C SST isotherm which creates the most productive tuna habitat where the chlorophyll front is in close proximity to the warm water SST (Fig. 7). This finding strengthens the hypothesis that the southward movement of the Oyashio Current likely induces migrations of forage of albacore such as the Pacific saury (Kimura *et al.*, 1997). It is important to stress that the southward displacement of tuna forage such as Pacific saury and squid corresponds to the development of albacore habitat. As a result, these can significantly increase albacore CPUE. The potential habitat may represent an optimum combination of biophysical environments for albacore ('frontal zones') where forage environments would be enhanced (Olson *et al.*, 1994; Zainuddin *et al.*, 2004).

Results of our study provide evidence for the high albacore concentrations in the specific area without any significant contribution from the oceanic front such as in November 1998 and November 2000. It suggests that the oceanographic features that defined the potential habitats for albacore between the period of 1998 and 2000 and that those in 1999 were different. To explore this subject, we used contour and eddy kinetic energy maps (Fig. 7). Our results showed that the high CPUEs formed in areas of the positive SSHA, on average, at approximately 13 cm and relatively high EKE in 1998 and 2000. We inferred from these results that the potential habitat corresponds to the areas of anticyclonically rotating eddies near the eastern Shatsky Rise area. The presence of meandering eddies likely trapped albacore prey transported by the KE to near the Shatsky Rise area (Komatsu *et al.*, 2002). Eddies generated from the Shatsky Rise presumably localize albacore forage and then create a good feeding opportunity for albacore. Another possible reason for the congregation of these species is the intrusion of the Oyashio Current, which transports albacore prey in the late fall (Kimura *et al.*, 1997). The eddy habitat produces locally elevated chlorophyll and zooplankton abundance, and mechanically affects local aggregation of prey organisms (Owen, 1981; Zhang *et al.*, 2001), and thereby stimulates feeding conditions (Logerwell and Smith, 2001).

Using statistical models, this study suggests that the albacore–environment relationship can be used to predict the spatial pattern of the region of highest albacore abundance (i.e., eddy fields and frontal zones). Our models indicate that the predicted areas of highest albacore abundance were consistent with the potential habitat on the simple prediction map and fishery observation data (Fig. 10), reflecting that spatial patterns of albacore distribution and abundance can be better predicted. In particular, the predicted areas of highest CPUEs corresponded well with the anticyclonic eddy field in November 1998 and in November 2000. In November 1999, the statistical models suggest that the predicted potential habitat for albacore associated strongly with frontal zones where warm water SST was in close proximity to the chlorophyll front.

Our prediction models were constructed using albacore CPUE–satellite-derived environmental data to find the key role controlling potential albacore habitats during the winter period. We then verified the model output generated from satellite-derived multiple oceanographic factors using sampling fishing ground data in November as the highest CPUEs during the winter period occurred in this month. Thus, we feel our predictions have been substantially verified.

Overall, these results suggest that the frontal structures and eddy fields play an important role for stimulating potential albacore habitats. These habitats may account for significant biophysical responses for albacore to find prey abundance and physiologically suitable conditions (Sund *et al.*, 1981; Polovina *et al.*, 2001). The results of our model predict the spatial pattern of the potential albacore habitat in good agreement with the simple prediction map and observation data. These results also suggest that multispectrum satellite images provide useful information on detection and prediction of potential habitat for albacore.

ACKNOWLEDGEMENTS

We gratefully acknowledge the Remote Sensing System for providing the TRMM/TMI SST data sets through Website (http://www.remss.com). The altimetry data used are produced by Ssalto/Duacs and distributed by Aviso, with support from Cnes. This work was partly supported to M.Z. by the Sasakawa Scientific Research Grant Number 16-416 M from the Japan Science Society. We also thank Dr Hidetada Kiyofuji for many helpful discussions.

REFERENCES

Andrade, H.A. and Garcia, A.E. (1999) Skipjack tuna in relation to sea surface temperature off the southern Brazilian coast. *Fish. Oceanogr.* **8:**245–254.

Bhat, G.S., Vecchi, G.A. and Gadgil, S. (2004) Sea surface temperature of the Bay of Bengal derived from the TRMM Microwave Imager. *J. Atmos. Ocean. Technol.* **21:**1283–1290.

Hastie, T.J. and Tibshirani, R.J. (1990) *Generalized Additive Models*. London: Chapman and Hall

Kimura, S., Nakai, M. and Sugimoto, T. (1997) Migration of albacore, *Thunnus alalunga*, in the North Pacific Ocean in relation to large oceanic phenomena. *Fish. Oceanogr.* **6:**51–57.

Komatsu, T., Sugimoto, T., Ishida, K., Itaya, K., Mishra, P. and Miura, T. (2002) Importance of the Shatsky Rise area in the Kuroshio Extension as an offshore nursery ground for Japanese anchovy (*Engraulis japonicus*) and sardine (*Sardinops melanostictus*). *Fish. Oceanogr.* **11:**354–360.

Laurs, R.M. and Lynn, R.J. (1991) North Pacific albacore ecology and oceanography. In: *Biology, Oceanography and Fisheries and the North Pacific Transition Zone and Subarctic Frontal Zone*. J.A. Wetherall (ed.) Honolulu: NOAA Technical Report NMFS, pp. 69–87.

Laurs, R.M., Fielder, P.C. and Montgomery, D.R. (1984) Albacore tuna catch distributions relative to environmental features observed from satellites. *Deep Sea Res.* **31:**1085–1099.

Lehodey, P., Bertignac, M., Hampton, J., Lewis, A. and Picaut, J. (1997) El Niño southern oscillation and tuna in the western Pacific. *Nature* **389:**715–718.

Logerwell, E.A. and Smith, P.E. (2001) Mesoscale eddies and survival of life stage Pacific sardine (*Sardinop sagax*) larvae. *Fish. Oceanogr.* **10:**13–25.

Mathsoft. (1999) *S-Plus 2000 guide to statistics*. Seattle: Data Analysis Products Division, Mathsoft, Inc.

McClain, C.R., Cleave, M.L., Fieldman, G.C., Gregg, W.W., Hooker, S.B. and Kuring, N. (1998) Science quality SeaWiFS data for global biosphere research. *Sea Technol.* **39:**10–16.

McCullagh, P. and Nelder, J.A. (1989) *Generalized Linear Models*. London: Chapman & Hall

Montañez, J.A.D., Buenrostro, A.A., Aguilar, S.M. and Almazan, A.M. (2004) Spatial analysis of yellowfin tuna (*Thunnus albacores*) catch rate and its relation to El Niño and La Niña events in the eastern tropical Pacific. *Deep Sea Res.* **51:**576–586.

Olson, R.J. and Boggs, C.H. (1986) Apex predation by yellowfin tuna (*Thunnus albacores*): independent estimates from gastric evacuation and stomach contents, bioenergetics and cesium concentrations. *Can. J. Fish. Aquat. Sci.* **43:**1760–1755.

Olson, D.B., Hitchcock, J.A., Mariano, A.J. *et al.* (1994) Life on the edge: marine life and fronts. *Oceanography* **7:**52–60.

Owen, R.W. (1981) Fronts and eddies in the sea: mechanisms, interaction and biological effects. in: *Analysis of Marine Ecosystem*. A.R. Longhurst (ed.) New York: Academic Press, pp.197–234.

Perry, R.I. and Smith, S.J. (1994) Identifying habitat associations of the marine fishes using survey data: an application to the northwest Atlantic. *Can. J. Fish. Aquat. Sci.* **51:**589–602.

Polovina, J.J., Kleiber, P. and Kobayashi, D.R. (1999) Application of TOPEX/POSEIDON satellite altimetry to simulate transport dynamics of larvae of spiny lobster, *Panulirus marginatus*, in the northwestern Hawaiian Islands, 1993–1996. *Fish. Bull.* **97:**132–143.

Polovina, J.J., Howel, E., Kobayashi, D.R. and Seki, M.P. (2001) The transition zone chlorophyll front, a dynamic global feature defining migration and forage habitat for marine resources. *Prog. Oceanogr.* **49:**469–483.

Polovina, J.J., Balazs, G.H., Howell, E.A., Parker, D.M., Seki, M.P. and Dutton, P.H. (2004) Forage and migration habitat of loggerhead (*Caretta caretta*) and olive ridley (*Levidochelys olivacea*) sea turtles in the central North Pacific Ocean, *Fish. Oceanogr.* **13:**36–51.

Robinson, I.S. (2004) *Measuring the ocean from space: The principles and methods of satellite oceanography*. Chichester: Praxis Publishing, Springer

Roden, G.I. (1991) Subarctic-subtropical transition zone of the North Pacific: large-scale aspects and mesoscale structure. In: *Biology, Oceanography and Fisheries of the North Pacific Transition Zone and Subarctic Frontal Zone*. J.A. Wetherall (ed.) Honolulu: NOAA Technical Report NMFS, **105**, pp. 1–38.

Schick, R.S., Goldstein, J. and Lutcavage, M.E. (2004) Bluefin tuna (*Thunnus thynnus*) distribution in relation to sea surface temperature fronts in the Gulf of Maine (1994–96). *Fish. Oceanogr.* **13:**225–238.

Sund, P.N., Blackburn, M. and Williams, F. (1981) Tuna and their environment in the Pacific Ocean: a review. *Oceanogr. Mar. Biol. Annu. Rev.* **19:**443–512.

Testut, C.E., Brankart, J.M., Brasseur, P. and Verron, J. (2003) Assimilation of sea surface temperature and altimetric observations during 1992–1993 into an eddy permitting primitive equation model of the North Atlantic Ocean. *J. Mar. Sys. 40* **41:**291–316.

Uda, M. (1973) Pulsative fluctuation of oceanic fronts in association with tuna fishing ground and fisheries. *J. Fac. Mar. Sci. Technol., Tokai Univ.* **7:**245–265.

Wentz, F.J., Gentenmann, C., Smith, D. and Chelton, D. (2000) Satellite measurements of sea surface temperature through clouds. *Science* **288:**847–850.

Zainuddin, M., Saitoh, K. and Saitoh, S. (2004) Detection of potential fishing ground for albacore tuna using synoptic measurements of ocean color and thermal remote sensing in the northwestern North Pacific. *Geophys. Res. Lett.* **31:**L20311; doi:10.1029/2004GL021000.

Zhang, J.Z., Wanninkhof, R. and Lee, K. (2001) Enhanced new production observed from the diurnal cycle of nitrate in an oligotrophic anticyclonic eddy. *Geophys. Res. Lett.* **28:**1579–1582.